Bioorganic & Medicinal Chemistry 18 (2010) 6170–6178

Contents lists available at ScienceDirect

Bioorganic & Medicinal Chemistry

journal homepage: www.elsevier.com/locate/bmc

# New porphyrin amino acid conjugates: Synthesis and photodynamic effect in human epithelial cells

V. Vaz Serra [a,†], A. Zamarrón [b,†], M. A. F. Faustino [a], M. C. Iglesias-de la Cruz [b], A. Blázquez [b], J. M. M. Rodrigues [a], M. G. P. M. S. Neves [a], J. A. S. Cavaleiro [a,*], A. Juarranz [b], F. Sanz-Rodríguez [b,*]

[a] QOPNA & Department of Chemistry, University of Aveiro, 3810-193 Aveiro, Portugal
[b] Departamento de Biología, Facultad de Ciencias, Universidad Autónoma de Madrid, 28049 Madrid, Spain

ARTICLE INFO

*Article history:*
Received 8 April 2010
Revised 9 June 2010
Accepted 10 June 2010
Available online 17 June 2010

*Keywords:*
Porphyrins
Amino acids
Photodynamic therapy
HeLa cells
HaCat cells

ABSTRACT

The efficacy of new porphyrin amino acid conjugates as photosensitizers for photodynamic therapy (PDT) were assayed in vitro on tumoral (HeLa) and on non tumoral (HaCaT) human cell lines. The conjugates stable in liposomes are able to penetrate efficiently in the cytoplasm of cultured cancer and normal cells. No dark cytotoxicity is observed at the same concentration used for PDT cell treatment and during long incubation time (24 h). The cell survival after the PDT treatment with visible light is dependent upon light exposure level and compound concentration. The tested compounds show higher photocytotoxicity in tumoral HeLa cells than in no tumoral HaCaT cells. The results suggest that these amino acid porphyrin conjugates are potential photosensitizers for PDT.



## 1. Introduction

Photodynamic therapy (PDT) is an alternative treatment for cancer and non-cancerous lesions. Malignant and abnormal cells are destroyed by singlet oxygen and by reactive oxygen species that are generated by a photosensitive drug (photosensitizer) when light of appropriate wavelength is applied.[1,2] PDT exhibits several advantages over surgery, chemotherapy, and radiotherapy, the standard modalities of tumor treatment. It is minimally invasive, devoid of severe side effects, yields a good cosmetic result, and often improves the patient's quality of life.[3]

Porphyrins, due to their unique photophysical and photochemical properties, have a special relevance in photodiagnosis (PD) and in photodynamic therapy (PDT) of oncologycal and non oncologycal diseases. In the last decades, a large number of porphyrins and porphyrin analogues (e.g., chlorins and phthalocyanines) have been extensively exploited as photosensitizers (PS). Some commercially available PS formulations that are currently in clinical practice are based in this type of macrocycles.[4–7] Porphyrin precursors like 5-aminolevulinic acid (ALA) that generates endogenously protoporphyrin IX, has been also widely used as a prodrug for PDT.[8] The ideal molecule to be used as PS should exhibit a low level of dark and systemic toxicity, good tumor selectivity avoiding accumulation in the surrounding healthy tissues, and should be rapidly eliminated from the organism to prevent prolonged photosensitivity.[7,9] With the aim to increase the biological effectiveness of porphyrin as photosensitizers their conjugation to different molecules, like proteins,[10–13] peptides,[14–17] and sugars[18] have been investigated in recent years. In particular, some porphyrins coupled with amino acids have also been reported to have interesting characteristics for PDT. Some of these porphyrins are able to intercalate DNA sequences with high specificity[19,20] and to enhance the cellular uptake in tumors.[11] They have good solubility in aqueous solutions and also possible specific interactions with cell membranes.[21,22] Remarkable photocytotoxicity after visible light irradiation is also reported for this kind of conjugates.[23] Recent studies, based on poly-*S*-lysine and meso-tetraarylporphyrins conjugates reveal that they are efficient in the photoinactivation of antibiotic resistant Gram-positive and Gram-negative bacteria. Other porphyrin analogues, like chlorin $e_6$, coupled to poly-*S*-lysine are also effective in the photoinactivation of these bacteria strains.[25,26] Knowing that amino acid moieties improve the solubility in aqueous solutions and are able to stablish specific interactions with cell membranes, porphyrins with amino acid moieties may be a good candidates for PDT.

As part of a program related with the development of new compounds with potentiality to be used in medicine[24,27–29] we report here the synthesis, structural and photophysical characterization

* Corresponding authors. Tel./fax: +34 914978243 (F.S.-R.); tel.: +351 234370717; fax: +351 234370084 (J.A.S.C.).
*E-mail addresses:* jcavaleiro@ua.pt (J.A.S. Cavaleiro), francisco.sanz@uam.es, brig96@hotmail.com (F. Sanz-Rodríguez).
† Both authors contributed equally to this work.

0968-0896/$ - see front matter © 2010 Elsevier Ltd. All rights reserved.
doi:10.1016/j.bmc.2010.06.030

of a series of porphyrin derivatives conjugated with commercial available amino acid residues. The photodynamic effect of the stable conjugates was evaluated on tumoral (HeLa) and no tumoral (HaCaT) human cells in culture. The dark toxicity, phototoxicity, intracellular localization of the PSs, and also the changes in morphology of cells induced by the photodynamic treatment will be presented and discussed.

## 2. Results and discussion

### 2.1. Chemistry

#### 2.1.1. Synthesis of porphyrin amino acid conjugates

Based on the knowledge that porphyrins with *meta*-methoxyphenyl groups in meso positions show high cellular uptake[28,29] we have chosen porphyrin **1** as the porphyrin moiety to be used in the preparation of the porphyrin amino acid conjugates **3–6** (Scheme 1). The presence of the carboxyl group on one of the phenyl substituents appears to us, an easy option to connect porphyrin **1** through an amide linkage to simple and commercially available amino acids.

Porphyrin **1**, with 3-methoxyphenyl and 4-carboxyphenyl *meso*-substituents was synthesized by condensation of pyrrole with 3-methoxybenzaldehyde and 4-formylbenzoic acid (3:1) in a refluxing mixture of acetic acid and nitrobenzene, as generally described in the Rothemund modified procedure.[24,30] This reaction afforded porphyrin 1 after purification by silica gel chromatography. The synthetic strategy used for the coupling of porphyrin **1** to the amino acid moiety is summarized in Scheme 1. In our first synthetic approach, the activation of the carboxylic function was performed with thionyl chloride in dry pyridine, yielding the corresponding porphyrinic acyl chloride. Due to the poor solubility of the amino acid moiety, its direct addition to the porphyrinic acyl chloride solution did not afforded the desired product. Further addition of *N*-hydroxysuccinimide at 50 °C afforded the activated ester **2** (Scheme 1). After the work up, porphyrin **2** was obtained in 97% yield. The porphyrin amino acid conjugates were prepared by reacting each amino acid with porphyrin **2**, in the presence of an excess of $K_2CO_3$ (Scheme 1). After stirring over night at 40 °C in DMSO, washing with water, drying and rapid column chromatography on silica gel, the new products were obtained from moderate (51% for derivative **5**) to excellent yields (>90% for porphyrins **3**, **4**, and **6**). The structures of all the new compounds were confirmed by NMR spectroscopy ($^1$H, $^{13}$C, COSY, HSQC, HMBC), elemental analysis, MS and UV–vis techniques. An extensive study on the characterization of these porphyrins by electrospray ionization tandem mass spectrometry (ESI-MS/MS) was already reported by our group.[31]

The $^1$H NMR spectra confirms that the obtained derivatives are *meso*-substituted porphyrin derivatives, showing the resonances of all the eight β-pyrrolic protons as multiplets ($\delta$ 8.77–8.91). The resonances of all the protons of the meso positions also appear at characteristic chemical shifts. The *para* substitution of one of the porphyrinic phenyl rings is also in accordance with the $^1$H NMR assignments: (i) the resonances of the *meta* and *ortho* protons appears as doublets at $\delta$ 8.20–8.25 and $\delta$ 8.28–8.32 (except for

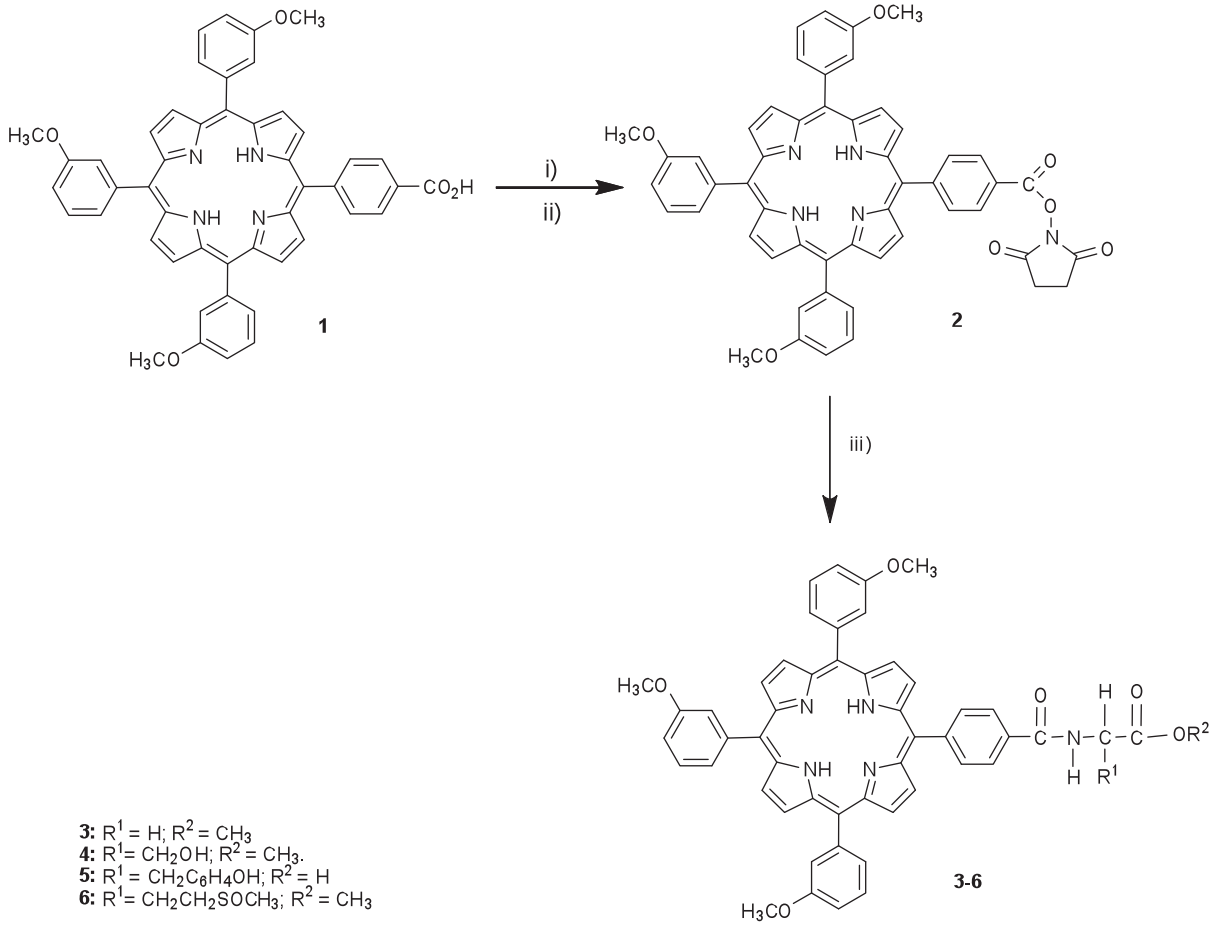


**3:** $R^1$ = H; $R^2$ = $CH_3$
**4:** $R^1$ = $CH_2OH$; $R^2$ = $CH_3$.
**5:** $R^1$ = $CH_2C_6H_4OH$; $R^2$ = H
**6:** $R^1$ = $CH_2CH_2SOCH_3$; $R^2$ = $CH_3$

**Scheme 1.** Reagents and conditions: (i) $SOCl_2$, dry py, rt; (ii) *N*-hydroxysuccinimide, 50 °C; (iii) $NH_2CHR^1CO_2R^2$, DMSO, $K_2CO_3$, 40 °C.

compound **5** where these resonances appears as a multiplet); (ii) it can be distinguished the typical resonances of only three protons of the *para* positions. The linkage of the amino acid residue through an amide linkage is also confirmed by the resonance of the proton of the amide group as a triplet at $\delta$ 6.98 for compound **3**. For compounds **4**, **5**, and **6** the resonance of this proton appears as duplets at $\delta$ 7.44, 8.37, and 7.88, respectively. Along with the several common resonance signals that reflect their common structural features, distinct resonance signs depending on the chemical structure of the amino acid moiety can also be distinguished. In particular, the resonance of the proton of the hydroxyl group for compounds **4** and **5**. The COSY spectrum of compound **4** allowed us to identify that resonance to the multiplet at $\delta$ 2.58–2.62 due to the existence of only one correlation sign with the multiplet at $\delta$ 4.22–4.25 assigned as the resonance of the $CH_2$. For compound **5**, the HSQC spectrum allowed the unequivocal identification of the signals of the aromatic carbons of the amino acid residue at $\delta$ 130.3 for C-6″ and C-10″ and at $\delta$ 114.8 for C-7″ and C-9″. The HMBC spectrum allowed us to identify the resonance of the proton of the hydroxyl group at $\delta$ 9.19 due to the long distance coupling ($^3J$) between this proton and C-7″ and C-9″.

The porphyrin **1** shows a typical ethio-type visible spectrum, with an intense band centered at 419 nm (Soret band) and the four Q bands at 514, 548, 587, and 645 nm. The insertion of the amino acid moiety does not introduce significant changes in the UV–vis spectrum of the new derivatives **3**–**6**.

It is interesting to note that all the attempts to obtain the non oxidized porphyrin–methionine conjugate were unsuccessful. The $FAB^+$ spectra of the derivative **6** clearly support the oxidized structure proposed, showing a molecular ion $[M+H]^+$ at *m/z* 910.

### 2.1.2. Photostability of the compounds

The rate of photodegradation exhibit by a compound under light conditions is a very important parameter to assess when we consider their potential application as photosensitizer. Porphyrin derivatives can go through photobleaching when exposed to UV–vis light and oxygen.[32] A fast photobleaching would cause the concentration of the drug to decrease, thus impairing the effectiveness of the treatment. To induce photobleaching, aerated solutions of compounds **3**–**6** in DMF, under magnetic stirring, were irradiated with white light at a fluence rate of 9.15 mW/cm$^2$. The UV–vis spectra were recorded at different times of irradiation (0, 1, 2, 3, 4, 6, 8, 11, 15, and 20 min) and the absorbance intensity of the Soret band was monitored and compared with the original one. The UV–vis spectra of all target compounds did not show any absorbance decay of the Soret and Q bands, during the total irradiation period. As an example, the UV–vis spectra of compound **3** at two different irradiation times are shown in Figure 1. The results point out that all studied compounds are highly stable under such conditions.

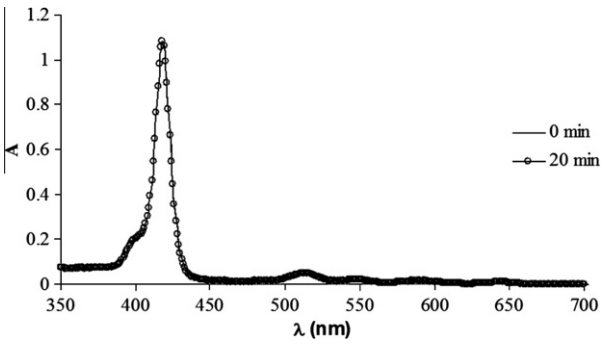


**Figure 1.** UV–vis spectra of compound **3** (DMF) after irradiation (white light, 9.15 mW/cm$^2$) at 0 and 20 min (total light dose 11 J/cm$^2$).

### 2.1.3. Singlet oxygen production measurement

Today, it is well accepted that singlet oxygen plays a key role in cell death induced by PDT. Considering the potential application of the porphyrin amino acid conjugates **3**–**6** in PDT, we evaluated their ability to generate singlet oxygen. The ability of these porphyrin derivatives to generate singlet oxygen, the basis of the photoinactivation process, was qualitatively evaluated by monitoring the photodecomposition of 1,3-diphenylisobenzofuran (DPBF). The production of singlet oxygen was established qualitatively using DPBF as a singlet oxygen quencher.[33–35] Solutions of DPBF (50 μM) and of the porphyrinic compounds (0.5 μM) in DMF were irradiated, over a total period of 15 min, in glass cuvettes with light at a fluence rate of 9.15 mW/cm$^2$. The light beam was previous filtered using a cut-off filter ($\lambda$ <550 nm) in order to remove all high-energy wavelengths. The photodecomposition of DPBF was monitored by measuring the decreasing of the absorbance at 414 nm registered in 15 seconds intervals of irradiation and the results are reported in Figure 2. The porphyrin 5,10,15,20-tetraphenylporphyrin (TPP) that is considered a good singlet oxygen producer, was used as a reference.[36] The DPBF photodegradation is higher in the presence of all the photosensitizers and the decay curves of all the compounds are quite comparable to TPP. On the other hand, the DPBF decay rate is higher in the presence of the porphyrin amino acid conjugate **4**, denoting in this case a higher efficiency to generate singlet oxygen under the same experimental conditions than TPP.

## 2.2. Studies in vitro on HaCaT and HeLa cells

### 2.2.1. Cell viability

The potentiality of the porphyrin amino acid conjugates **3**–**6** as photosensitizers was tested using HeLa human cervical cancer cell line and HaCaT human normal skin keratinocytes cell line. The cytotoxic activity of the conjugates was evaluated using the MTT assay. Different concentrations of the porphyrin conjugates **3**–**6** ($1.2 \times 10^{-5}$–$2.2 \times 10^{-7}$ M) were administered to cell cultures in liposomal solutions and the cells were incubated, in the dark, for a period of 4 h. The cytotoxicity and the photocytotoxicity of compound **5** were not determined because its incorporation into phospholipids layers was not successful even after several attempts. The survival rates obtained (Table 1) show that no significant dark cytotoxicity is observed at concentrations up to $2.4 \times 10^{-6}$ M.

For the photodynamic assays, the cell cultures were incubated for a period of 4 h in the presence of non cytotoxic concentrations of porphyrin conjugates and then submitted to different times of irradiation with red light (5, 10, and 20 min) with a fluence rate of 9.15 mW/cm$^2$. The results obtained for the cell survival,

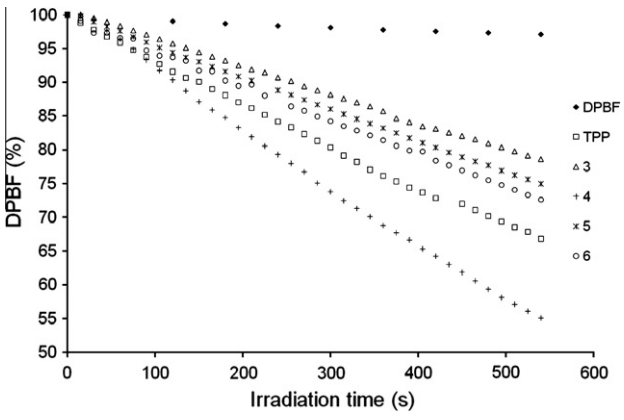


**Figure 2.** Comparative photooxidation of DPBF (50 μM) in DMF with or without photosensitizer (0.5 μM); white light (9.15 mW/cm$^2$) filtered through a cut-off filter $\lambda$ <550 nm.

**Table 1**
Percent survival of two cell lines, HeLa and HaCaT, incubated in the dark for a period of 4 h at different concentrations of compounds **3**, **4**, and **6**

| Entry | Compound | Concentration (M) | Surviving fraction (% ± SD) | |
|---|---|---|---|---|
| | | | HaCaT | HeLa |
| 1 | **3** | $2.2 \times 10^{-7}$ | 94.98 ± 5.21 | 107.31 ± 2.73 |
| | | $6.1 \times 10^{-7}$ | 97.96 ± 6.26 | 110.38 ± 3.37 |
| | | $1.2 \times 10^{-6}$ | 102.19 ± 8.01 | 106.97 ± 6.64 |
| | | $2.4 \times 10^{-6}$ | 109.91 ± 5.0 | 104.89 ± 8.81 |
| | | $1.2 \times 10^{-5}$ | 24.30 ± 2.47 | 60.42 ± 3.62 |
| 2 | **4** | $2.2 \times 10^{-7}$ | 101.49 ± 1.2 | 102.58 ± 1.36 |
| | | $6.1 \times 10^{-7}$ | 104.72 ± 4.49 | 100.28 ± 1.26 |
| | | $1.2 \times 10^{-6}$ | 102.65 ± 2.98 | 102.78 ± 0.09 |
| | | $2.4 \times 10^{-6}$ | 97.54 ± 12.0 | 91.48 ± 0.23 |
| | | $1.2 \times 10^{-5}$ | 96.98 ± 11.54 | 67.33 ± 8.51 |
| 3 | **6** | $2.2 \times 10^{-7}$ | 99.20 ± 6.70 | 93.26 ± 9.66 |
| | | $6.1 \times 10^{-7}$ | 101.50 ± 6.60 | 92.61 ± 5.04 |
| | | $1.2 \times 10^{-6}$ | 103.40 ± 4.90 | 95.69 ± 4.81 |
| | | $2.4 \times 10^{-6}$ | 101.30 ± 12.70 | 93.50 ± 9.18 |
| | | $1.2 \times 10^{-5}$ | 16.90 ± 3.35 | 16.93 ± 3.17 |

Each point corresponds to the mean value ± SD from three different experiments.

summarized in Table 2, show that the cell photokilling is dependent on both the photosensitizer concentration and the irradiation time. A significant photocytotoxicity (survival fractions of about 20%) can be observed on non tumoral HaCaT cells when the photosensitizers **4** and **6** were used at concentration $1.2 \times 10^{-6}$ M and after 20 min of irradiation. Furthermore, 100% lethality can be observed for compound **3** under the same conditions ($1.2 \times 10^{-6}$ M, 20 min of irradiation). The phototoxic effect is less pronounced at lower concentrations and shorter irradiation times (Table 2). For example, a high HaCaT cell survival percentage of 82.69 ± 0.01% and 76.87 ± 5.58% can be reached with compounds **3** and **6** at concentrations of $2.5 \times 10^{-7}$ and $3.0 \times 10^{-7}$ M, respectively, after 5 min of irradiation. Furthermore, no photocytotoxicity on HaCaT cells is observed with compound **4** at $6.1 \times 10^{-7}$ M and after 20 min of irradiation with red light. It is interesting to note that compounds **3** and **4** at concentrations of $2.5 \times 10^{-7}$ and $1.2 \times 10^{-6}$ M, respectively, show significant phototoxicity in HeLa cells upon 5 min of irradiation; only surviving cells fractions of 3.74 ± 3.40% (compound **3**) and 8.00 ± 3.90% (compound **4**) are observed. A less pronounced phototoxic effect (56.87 ± 3.81) is detected for compound **6** at $3.0 \times 10^{-7}$ M and after 5 min. These results, point out that compounds **3** and **4** provide a good photodynamic effect in HeLa cells with minimal photocytotoxicity to non tumoral cells at concentrations of $2.5 \times 10^{-7}$ and $1.2 \times 10^{-6}$ M.

### 2.2.2. Subcellular localization and morphological studies

The subcellular localization experiments and morphological studies were conduced under sublethal conditions ($LD_{50}$) for the non tumoral HaCaT cells. So the conditions selected were: (i) $2.5 \times 10^{-7}$ M for compound **3** (cell survival of 50.96 ± 1.3%); (ii) $1.2 \times 10^{-6}$ M for compound **4** (cell survival of 42.75 ± 1.5%); (iii) $3.0 \times 10^{-7}$ M for compound **6** (cell survival of 53.02 ± 8.4%) and 10 min of red light irradiation. Figure 3 shows that $LD_{50}$ conditions for the non tumoral HaCaT cells, induced a 100% lethality in the tumoral HeLa cells.

Morphologically, HaCaT cells tend to form microcolonies with well developed adhesion systems. At $LD_{50}$ conditions the cells retained the morphology quite similar to that control cells for all the studied conjugates after 10 min of irradiation (Fig. 4A–D). However, after 20 min of irradiation cells showed a partial retraction, loss of adhesion and cytoplasmic vacuolization (Fig. 4E–H). These effects were more evident at the edge of the colonies than in the center of them, because cells located at the edge of colonies were more exposed to photosensitizers. PDT treatments induced also morphological changes in HeLa cells, but substantially different to those observed in HaCaT cells. Figure 4J, K shows some morphological changes for compound **3** and **4** after 2 min of irradiation. These alterations are more evident under $LD_{50}$ conditions for HeLa cells. (data not shown because after 10 min of PDT almost 100% of the cells were dead). $LD_{50}$ of derivative **6** (Fig. 4L), produced in HeLa cells a drastic effect such as cytoplasmic vacuolization, followed by loss of adhesion and loss of basophilia, which was more evident after 10 min of light irradiation.

To analyze the intracellular localization of the amino acids conjugates, the cells were incubated up to 24 h at the $LD_{50}$ selected concentration for HaCat in order to visualize the time-dependent changes in intracellular localization of the PSs. For this purpose, cells were incubated with compound **3** ($2.5 \times 10^{-7}$ M), **4** ($1.2 \times 10^{-6}$ M), and **6** ($3.0 \times 10^{-7}$ M) for 6 h and 24 h, respectively. In HaCaT cells, all the compounds were concentrated mainly within the cells and appeared as different size granules fitting the distribution pattern of lysosomes (Fig. 5).

In the same figure it can be observed that the PSs exhibit different localization patterns in HeLa cells; conjugate is located at lysosomes, and compounds **4** and **6** are located in the plasma membrane at both studied incubation times (6 h and 24 h). We did not see any localization patterns characteristic for mitochondria (blue signal Fig. 5).

It is known that effective photodamage of PSs in both cell cultures and tumors is related to the chemical structure, concentration, incubation time, vehicle, light dose, and site of subcellular localization. Several cell components have been described as targets for the cytotoxic effects of ROS (reactive oxygen species) including mitochondria, lysosomes, Golgi apparatus, plasma membrane and nuclei. PSs localized in mitochondria and lysosomes are highly effective for cell photodamage, triggering either apoptotic or necrotic cell death responses.[37]

**Table 2**
Percent survival of two cell lines, HeLa and HaCaT, at different times of irradiation with a fluence rate of 9.15 mW/cm$^2$ and at different concentrations of compounds **3**, **4**, and **6**

| Entry | Compound | Concentration (M)s | Irradiation time (min) | Surviving fraction (% ± SD) | |
|---|---|---|---|---|---|
| | | | | HaCaT | HeLa |
| 1 | **3** | $2.5 \times 10^{-7}$ | 5 | 82.69 ± 0.01 | 3.74 ± 3.4 |
| | | | 10 | 50.96 ± 1.3 | 1.13 ± 0.5 |
| | | | 20 | 22.11 ± 1.3 | 1.32 ± 0.01 |
| 2 | **4** | $1.2 \times 10^{-6}$ | 5 | ND | 8.00 ± 3.9 |
| | | | 10 | 42.75 ± 1.5 | 0 |
| | | | 20 | 22.54 ± 3.0 | 0 |
| 3 | **6** | $3.0 \times 10^{-7}$ | 5 | 76.87 ± 5.58 | 56.87 ± 3.81 |
| | | | 10 | 53.02 ± 8.42 | 14.23 ± 1.50 |
| | | | 20 | 28.20 ± 1.66 | 10.93 ± 2.38 |

ND: not determined. Each point corresponds to the mean value ± SD from three different experiments.

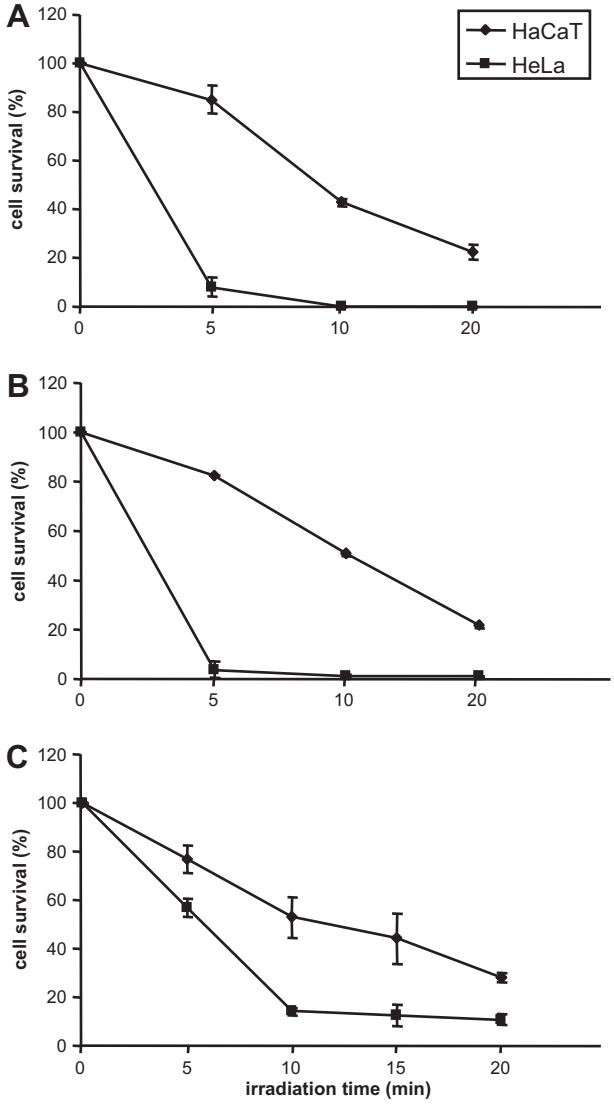


**Figure 3.** Photodynamic activity of porphyrin amino acid derivatives and effect of $LD_{50}$ treatments on HaCaT and HeLa cell lines. Cells were incubated for 4 h in the presence of $LD_{50}$ of (A) compound **3** ($2.5 \times 10^{-7}$ M), (B) compound **4** ($1.2 \times 10^{-6}$ M), and (C) compound **6** ($3.0 \times 10^{-7}$ M) and subjected to red light irradiation for variable times. Each points corresponds to the mean value ± SD from three different experiments.

In our study, we have seen that all the analyzed compounds are able to generate singlet oxygen, being compounds **4** and **6** the most efficient ones. Although compound **3** is the less efficient single oxygen producer, the fact that it is localized in lysosome membrane, instead of plasma membrane like the others two, can be responsible by its higher photocytotoxicity in tumoral cells.

In conclusion, four porphyrin amino acid conjugates **3**–**6** (glycine, serine, tyrosine and methionine residues) have been synthesized in good to excellent yields through an easy synthetic approach. All of the compounds show high photostability and are able to generate singlet oxygen. The conjugates **3**, **4**, and **6** show significant photocytotoxic activity in HaCaT and HeLa cell lines. Furthermore, the MTT cytotoxicity studies indicate that compound **3** had the highest efficacy at lower concentration. More, under $LD_{50}$ conditions for non tumoral cells (HaCaT) compound **3** produced 100% lethality in tumoral cells (HeLa). These facts, associated with the easy access to these porphyrin amino acid conjugates may provide valuable tools in PDT for the treatment of several diseases. Further in vitro studies concerning the mechanism of cell death produced by the photoactivation of these porphyrin amino acid conjugates are presently in progress in our laboratory.

## 3. Experimental

### 3.1. General

$^1$H and $^{13}$C NMR spectra were recorded in a Bruker AMX 300 NMR spectrometer (at 300.13 and 75.47 MHz, respectively): $CDCl_3$ was used as solvent and TMS as internal reference. The chemical shifts are expressed in $\delta$ (ppm) and the coupling constants ($J$) in Hertz (Hz). Mass spectra were recorded on VG AutoSpec Q mass spectrometer using $CHCl_3$ as solvent and 3-nitrobenzyl alcohol (NBA) as matrix. The UV–vis spectra were recorded on an UV-2501 PC Shimadzu spectrophotometer using DMSO as solvent. Melting points were measured on a Reichert Thermovar apparatus fitted with a microscope and are uncorrected. Analytical TLC was carried out on precoated sheets with silica gel (Merck, 60, 0.2 mm thick). Column chromatography was carried in silica gel (Merck, 230–400 mesh). Pyridine was distilled from potassium hydroxide, all other solvents and reagents were used without further purification. Dipalmitoyl D-α-phosphatidylcholine from Sigma was used in liposome preparation. The compounds purities were confirmed by thin layer chromatography, $^1$H NMR and elemental analysis.

#### 3.1.1. 5-(4-Carboxyphenyl)-10,15,20-tris(3-methoxyphenyl)-porphyrin (1)

4-Formylbenzoic acid (1.62 g, 10.8 mmol) and 3-methoxybenzaldehyde (2.63 mL, 21.6 mmol) were added to a refluxing mixture of glacial acetic acid (200 mL) and nitrobenzene (150 mL). After the dissolution of the 4-formylbenzoic acid, pyrrole (2.00 mL, 28.9 mmol) was added dropwise (ca. 4 min) to the mixture. The reaction mixture was then refluxed for 1 h. The solvents were distilled under reduced pressure and the crude material was taken into chloroform and directly chromatographed on a silica column using chloroform as eluent. The first fraction was identified as 5,10,15,20-tetrakis (3-methoxyphenyl) porphyrin. The second fraction, eluted with the same solvent, gave porphyrin **1** after evaporation of the solvent and recrystallization from chloroform/light petroleum. Yield: 8%. mp >300 °C. $^1$H NMR (300 MHz, $CDCl_3$): $\delta = -2.80$ (s, 2H, N*H*), 3.99 (s, 9H, 10,15,20-O*CH*$_3$-Ph), 7.34 (dd, $J = 8.2$ and 2.1 Hz, 3H, 10,15,20-H-*p*-Ph), 7.63–7.68 (m, 3H, 10,15,20-H-*m*-Ph), 7.79–7.83 (m, 6H, 10,15,20-H-*o*-Ph), 8.35 (d, $J = 7.6$ Hz, 2H, 5-H-*o*-Ph), 8.51 (d, $J = 7.6$ Hz, 2H, 5-H-*m*-Ph), 8.80 and 8.92 (AB, $J = 4.9$ Hz, 4H, H-β), 8.90 (s, 4H, H-β). MS (FAB$^+$) $m/z$: 749 [M+H]$^+$. UV–vis (DMSO): $\lambda_{max}$ (log $\varepsilon$) = 419 (5.66), 514 (4.28), 548 (3.92), 587 (3.78), 645 (3.72) nm.

#### 3.1.2. 5-[4-(Succinimide-*N*-oxycarbonyl)phenyl]-10,15,20-tris(3-methoxyphenyl)porphyrin (2)

To a stirred solution of porphyrin **1** (31 mg, 42 μmol) in dry pyridine was added $SOCl_2$ (0.1 mL, 163 mmol). The reaction mixture was maintained in the dark, protected from moisture with silica gel, during 30 min at room temperature. Then, *N*-hydroxysuccinimide (74 mg, 643 μmol) was added and the temperature rised to 50 °C. The reaction progress was monitored by TLC. When the reaction was complete (3 h), the solvent was removed under reduced pressure and the crude material was taken into chloroform. The mixture was neutralized with aqueous sodium hydrogencarbonate solution and extracted in chloroform. The organic layer was washed with water ($2 \times 100$ mL), dried over $Na_2SO_4$, and the solvent was removed. The residue was purified by flash chromatography (silica gel), using dichloromethane as eluent. Porphyrin **2** was crystallized

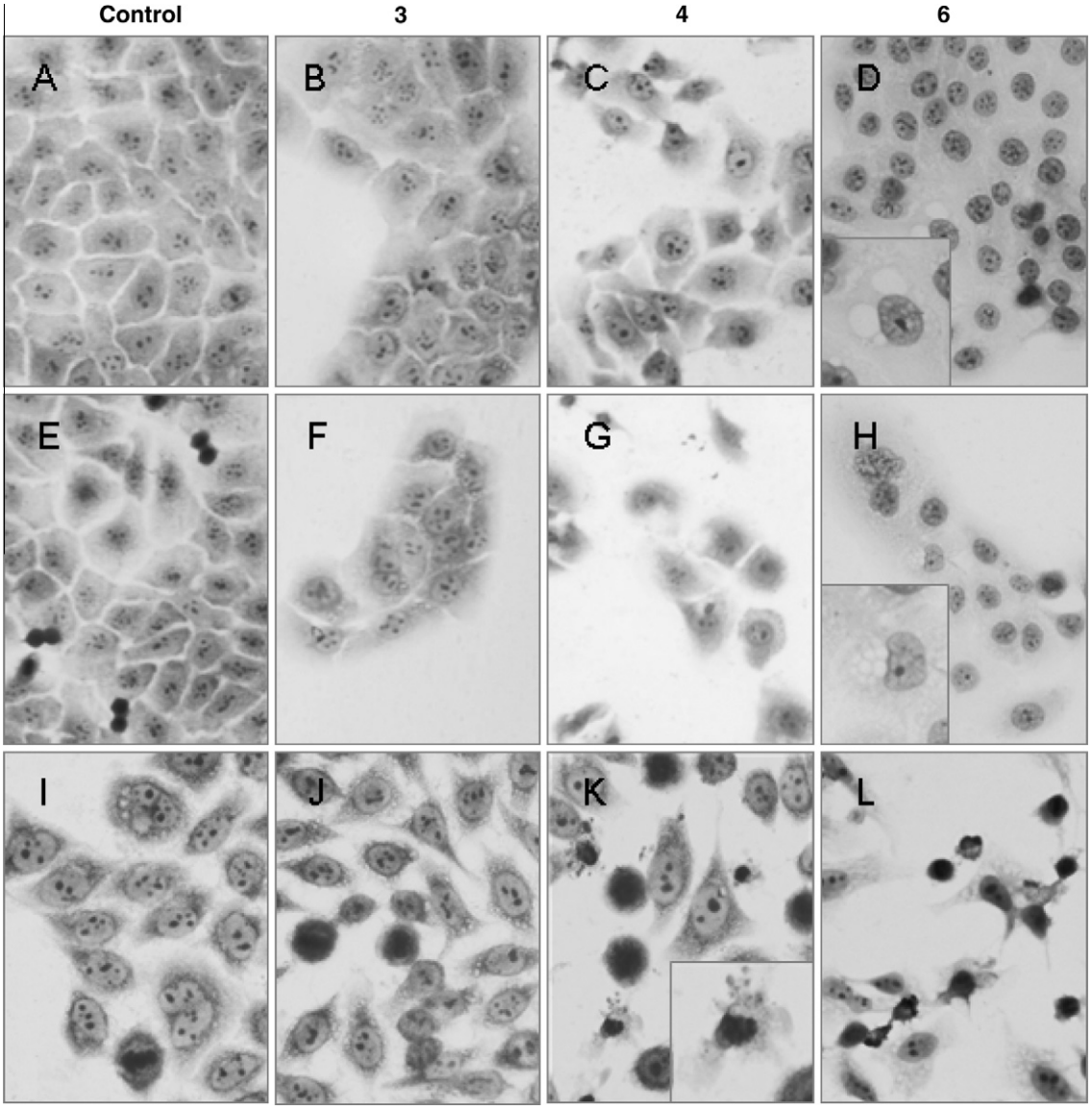


**Figure 4.** Morphological changes induced by porphyrin amino acid derivatives on HaCaT (A–H) and HeLa (I–L) cell lines when incubated for 4 h in the presence of compound **3** ($2.5 \times 10^{-7}$ M), **4** ($1.2 \times 10^{-6}$ M), and **6** ($3.0 \times 10^{-7}$ M). HaCat cells: A–D: 10 min of irradiation, E–H: 20 min of irradiation. HeLa cells: J, K: 2 min of irradiation, I, L: 10 min of irradiation. After light exposure, cells were fixed in cold methanol and stained with toluidine blue. Photographs are representative images of three different experiments for each compound.

from dichloromethane/light petroleum. Yield: 34.4 mg (97%). mp >300 °C. $^1$H NMR (300 MHz, $CDCl_3$): $\delta = -2.81$ (s, 2H, N*H*), 3.02 (s, 4H, C$H_2$), 3.99 (s, 9H, 10,15,20-OC$H_3$-Ph), 7.34 (dd, $J = 8.2$ and 2.1 Hz, 3H, 10,15,20-H-*p*-Ph), 7.63–7.68 (m, 3H, 10,15,20-H-*m*-Ph), 7.78–7.82 (m, 6H, 10,15,20-H-*o*-Ph), 8.38 (d, $J = 8.4$ Hz, 2H, 5-H-*o*-Ph), 8.55 (d, $J = 8.4$ Hz, 2H, 5-H-*m*-Ph), 8.76 (d, $J = 4.8$ Hz, 2H, H-β), 8.90 (s, 4H, H-β), 8.94 (d, 2H, $J = 4.8$ Hz, H-β). MS (FAB$^+$) *m/z*: 846 [M+H]$^+$. UV–vis (DMSO): $\lambda_{max}$ (log $\varepsilon$) = 419 (5.64), 514 (4.25), 548 (3.94), 587 (3.81), 645 (3.51) nm.

### 3.2. General procedure for the reaction of porphyrin 2 with amino acids

The amino acid (4 equiv) was dissolved in DMSO (2 mL) and then a large excess of $K_2CO_3$ and the activated ester **2** (1 equiv) were added. The reaction was kept overnight at 40 °C, under stirring, protected from light and from moisture with silica gel. Each organic layer was neutralized with citric acid, washed with water, extracted with dichloromethane, and dried over anhydrous sodium sulfate. After the reaction work up, the solvent was removed under pressure and each residue obtained was purified by flash chromatography using an appropriate solvent.

#### 3.2.1. Compound 3: MMA-Gly

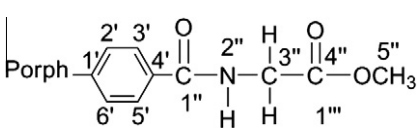


Yield: 93%. mp = 270–272 °C. $^1$H NMR (300 MHz, $CDCl_3$): $\delta = -2.81$ (s, 2H, N*H*), 3.90 (s, 3H, H-5″), 3.99 (s, 9H, OC$H_3$-Ph), 4.44 (d, $J = 4.9$ Hz, 2H, H-3″), 6.98 (t, $J = 4.9$ Hz, 1H, H-2″), 7.34 (dd, $J = 8.0$ and 2.0 Hz, 4H, H-*p*-Ph), 7.64 (t, $J = 8.0$ Hz, 3H, 10,15,20-H-*m*-Ph), 7.78–7.82 (m, 6H, 10,15,20-H-*o*-Ph), 8.20 (d, $J = 8.1$ Hz, 2H, 5-H-*m*-Ph), 8.31 (d, $J = 8.1$ Hz, 2H, 5-H-*o*-Ph), 8.77–8.91 (m, 8H, H-β). EM (FAB)$^+$ *m/z*: 819 [M+H]$^+$, 704 [M+H]$^+$:

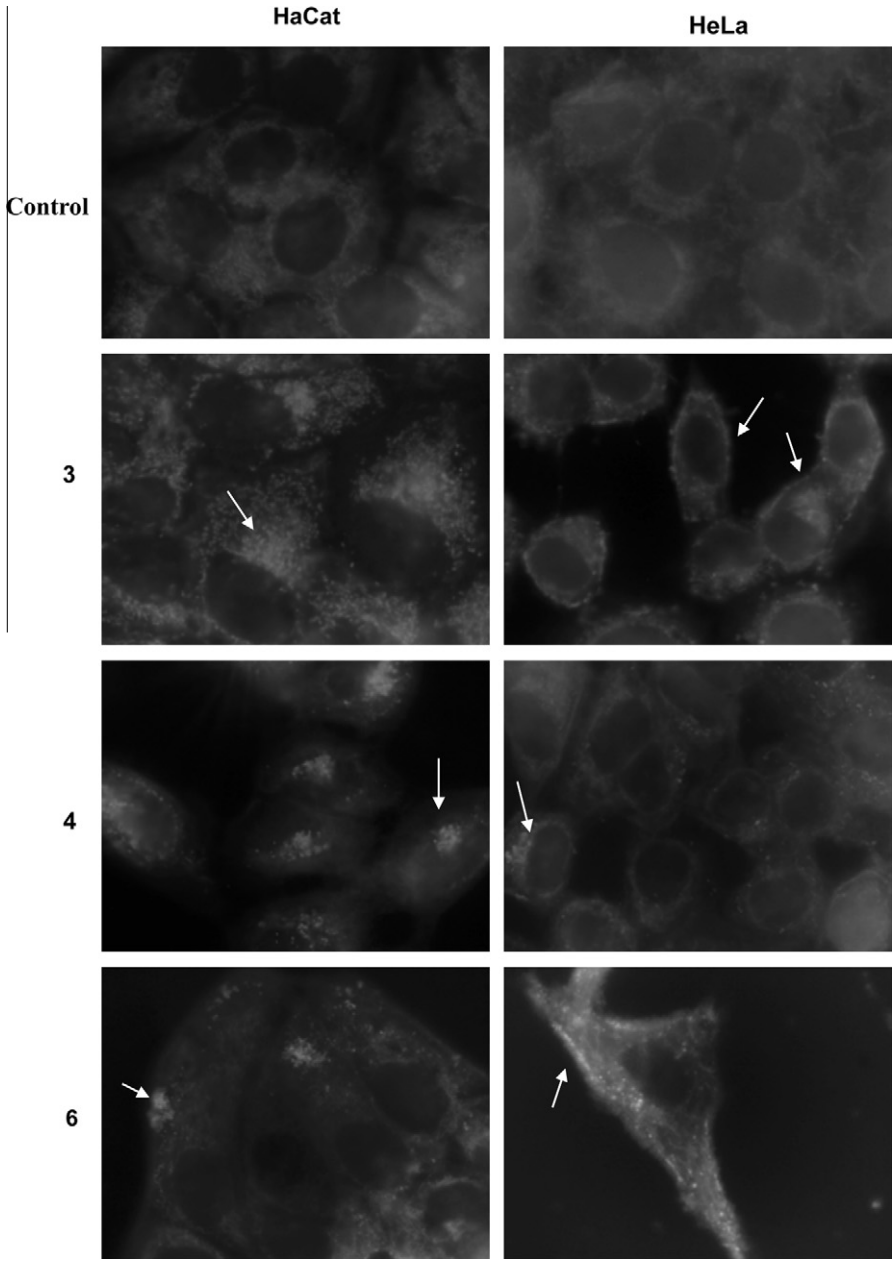


**Figure 5.** Intracellular localization of porphyrin amino acid derivatives in HaCaT and HeLa cells after incubation with each derivative for 6 h at concentration of $2.5 \times 10^{-7}$ M (**3**), $1.2 \times 10^{-6}$ M (**4**), and $3.0 \times 10^{-7}$ M (**6**) in complete medium. White arrows show the localization of the PSs those fluorescing in red and shown a lysosomal distribution. Blue autofluorescence of mitochondria's can be observed in both controls. Photographs concerning 24 h treatment are not shown due to similar pattern of PSs with 6 h treatment.

$C_4H_7NO_3$. UV–vis (DMSO): $\lambda_{max}$ (log $\varepsilon$) = 414 (5.70), 514 (4.32), 549 (3.90), 589 (3.79), 644 (3.61) nm. Anal. Calcd for $C_{51}H_{41}N_5O_6 \cdot H_2O$: C, 73.10; H, 5.17; N, 8.36. Found: C, 73.20; H, 5.07; N, 8.52.

### 3.2.2. Compound 4: MMA-Ser

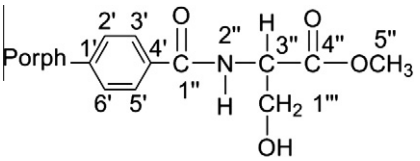


Yield: 91%. mp = 270–272 °C. $^1$H NMR (300 MHz, $CDCl_3$): $\delta$ = −2.81 (s, 2H, N*H*), 2.58–2.62 (m, 1H, Ser-O*H*), 3.93 (s, 3H, H-5″), 3.98 (s, 9H, 10,15,20-OC*H*$_3$-Ph), 4.22–4.25 (m, 2H, H-1‴), 5.07–5.10 (m, 1H, H-3″), 7.32–7.34 (m, 3H, 10,15,20-H-*p*-Ph), 7.44 (d, *J* = 7.1 Hz, 1H, H-2″), 7.64 (m, 3H, 10,15,20-H-*m*-Ph), 7.78 (s, 3H, 10,15,20-H-*o*-Ph), 7.80 (d, *J* = 7.1 Hz, 3H, 10,15,20-H-*o*-Ph), 8.25 (d, *J* = 8.0 Hz, 2H, 5-H-*m*-Ph), 8.32 (d, *J* = 8.0 Hz, 2H, 5-H-*o*-Ph), 8.78, 8.89, and 8.91 (d, s, d, *J* = 4.9 Hz, 8H, H-β). $^{13}$C NMR (75 MHz, $CDCl_3$): $\delta$ = 53.1 (C-5″), 55.4 (C-3″), 55.5 (10,15,20-O*C*H$_3$-Ph), 63.8 (C-1‴), 113.6 (10,15,20-C-*p*-Ph), 118.4 (Porf-C-5), 120.1, 120.2, 120.4 (10,15,20-C-*o*-Ph), 125.6 (5-C-*m*-Ph), 127.5 and 127.6 (10,15,20-C-*m*-Ph and 10,15,20-C-*o*-Ph), 131.3 (C-β), 132.8, 134.7 (5-C-*o*-Ph), 143.3, 146.2 (C-1′), 147.3, 157.9, 167.7 (C-1″). EM (FAB)$^+$ *m/z*: 850 [M+H]$^+$, 703 [M+H]$^+$: $C_5H_9NO_4$. UV–vis (DMSO): $\lambda_{max}$ (log $\varepsilon$) = 414 (5.70), 514 (4.33), 549 (3.91), 589 (3.79), 644 (3.64) nm. Anal. Calcd for $C_{52}H_{43}N_5O_7 \cdot H_2O$: C, 71.96; H, 5.23; N, 8.07. Found: C, 72.18; H, 5.23; N, 8.07.

### 3.2.3. Compound 5: MMA-Tyr

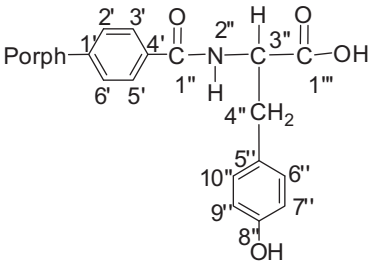

Yield: 51%. mp >300 °C. $^1$H NMR (300 MHz, $CDCl_3$): $\delta$ = −2.96 (s, 2H, Porf-N*H*), 3.07–3.18 (m, 2H, H-4″), 3.92 (s, 6H, 10,20-OC*H*$_3$-Ph), 3.95 (s, 3H, 15-OC*H*$_3$-Ph), 4.55 (br s, 1H, H-3″), 6.69 (d, *J* = 8.1 Hz, 2H, H-7″ and H-9″), 7.18 (d, *J* = 8.1 Hz, 2H, H-6″ and H-10″), 7.40 (dd, *J* = 11.8 and 9.1 Hz, 3H, 10,15,20-H-*p*-Ph), 7.63–7.67 (m, 9H, 10,15,20-H-*o*-Ph and 10,15,20-H-*m*-Ph), 8.20 (d, *J* = 7.8 Hz, 2H, H-3′ and H-5′), 8.28 (d, *J* = 7.8 Hz, 2H, H-2′ and H-6′), 8.37 (d, *J* = 5.6 Hz, 1H, H-2″), 8.83–8.87 (m, 8H, H-β), 9.19 (s, 1H, Tyr-O*H*). $^{13}$C NMR (75 MHz, $CDCl_3$): $\delta$ = 36.6 (C-4″); 55.4 (10,15,20-OC$H_3$-Ph); 56.4 (C-3″); 113.7 (10,15,20-*C*-*p*-Ph), 114.8 (C-7″ and C-9″); 119.1; 119.8; 119.9; 120.3 (10,15,20-*C*-*o*-Ph); 125.7 (C-3′ and C-5′); 127.2 (10,15,20-*C*-o-Ph); 127.9 (10,15,20-*C*-*m*-Ph); 128.9 (C-5″); 129.7 (C-8″); 130.3 (C-6″ and C-10″); 131.4 (C-β); 134.2 (C-2′, C-6′); 134.7 (C-5); 142.5; 143.8 (C-1′); 155.5; 157.7; 165.5 (*C*=O). EM (FAB)$^+$ *m/z*: 912 [M+H]$^+$, 704 [M+H]$^+$: $C_{10}H_{10}NO_4$. UV–vis (DMSO): $\lambda_{max}$ (log $\varepsilon$) = 418 (5.71), 514 (4.30), 549 (3.89), 588 (3.79), 644 (3.61) nm. Anal. Calcd for $C_{57}H_{45}N_5O_7{\cdot}3H_2O$: C, 70.87; H, 5.32; N, 7.25. Found: C, 70.76; H, 4.91; N, 6.88.

### 3.2.4. Compound 6: MMA-Met

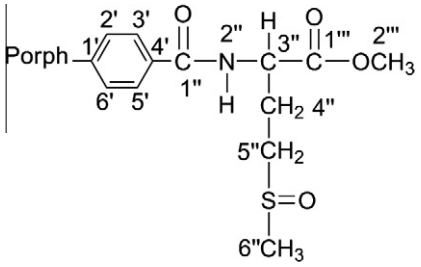

Yield: 90%. mp >300 °C. $^1$H NMR (300 MHz, $CDCl_3$): −2.82 (s, 2H, Porf-N*H*), 2.38–2.54, 2.84–2.92, 2.95–3.01, and 3.03–3.13 ppm (m, 4H, H-4″ and H-5″), 2.66 (s, 3H,H-6″), 3.91 (s, 3H, H-2‴), 3.99 (s, 3H, 10,15,20-OC$H_3$-Ph), 5.07–5.09 (m, 1H, H-3″), 7.34 (dd, *J* = 8.0 and 2.1 Hz, 3H, 10,15,20-H-*p*-Ph), 7.65 (t, *J* = 8.0 Hz, 3H, 10,15,20-H-*m*-Ph), 7.78–7.82 (m, 6H, 10,15,20-H-*o*-Ph) 7.88 (d, *J* = 7.0 Hz, 1H, H-2″), 8.26–8.33 (m, 4H, H-2′, H-3′, H-5′, H-6′), 8.78–8.91 (m, 8H, H-β).UV–vis (DMSO): $\lambda_{max}$ (log $\varepsilon$) = 419 (5.65), 513 (4.28), 548 (3.91), 588 (3.77), 645 (3.69) nm. EM (FAB)$^+$ *m/z*: 910 [M+H]$^+$, 703 [M+H]$^+$: $C_6H_{13}NO_4S$. HRMS (ESI) Calcd for $C_{53}H_{45}N_5O_7S$ [M+H]$^+$: $CH_3$: 895.3040, Found: 895.3026.

### 3.3. Singlet oxygen generation and photostability studies

Stock solution of each porphyrin derivative at 0.1 mM in DMF and a stock solution of 1,3-diphenylisobenzofuran (DPBF) at 10 mM in DMF were prepared.

The reaction mixture of 50 μM of DPBF and 0.5 μM of a porphyrin derivative in DMF in glass cells (2 mL) was irradiated with white light filtered through a cut-off filter of wavelength <550 nm, at a fluence rate of 9.15 mW/cm$^{-2}$. During the irradiation period, the solutions were stirred at room temperature. The generation of singlet oxygen was followed by its reaction with DPBF. The breakdown of DPBF was monitored by measuring the decreasing of the absorbance at 414 nm at irradiation intervals of 15 s. The photostability of the photosensitizers was determined by irradiating 2 mL of 1 μM solutions of the porphyrins in DMF with white light at a fluence rate of 9.15 mW/cm$^{-2}$. During such irradiation the solutions were magnetically stirred and kept at room temperature. At fixed intervals of time (0; 1; 2; 3; 4; 6; 8; 11; 15; 20 min), the concentration of the porphyrin was determined by visible absorption spectrophotometry.

### 3.4. Cell cultures

The HeLa human cervical cancer cell line and HaCaT human normal skin keratinocytes were stored frozen in liquid nitrogen. The cells were grown as a monolayer employing Dulbecco's Modified Eagle Medium (DMEM) containing 10% fetal calf serum (FCS) and 50 units/mL penicillin and 50 μg/mL streptomycin (Sigma). The cells were incubated at 37 °C in a humidified 5% $CO_2$ atmosphere and the medium was changed daily. For the photocytotoxicity experiments, cells were plated on 24-well plates and for fluorescence observation, cells were plated onto round coverslips placed into wells.

### 3.5. Preparation of liposomes

Since these porphyrin conjugates are not soluble in PBS or water, they were administered to cell cultures in liposomal solution. Each compound was dissolved in pyridine to a concentration of 0.5 mg/mL and stored in the dark at 4 °C until use. The incorporation of the sensitizers into liposomes of dipalmitoyl D-α-phosphatidylcholine (Sigma, St Louis, MO, USA) was carried out by the injection procedure as previously described.[38] Liposomal suspension of porphyrins amino acid conjugates were sterilized by filtration through a Millipore filter (0.22 μM of pore size) and used within 48 h after preparation. The concentration of the three photosensitizers was estimated by the absorbance at the Soret band using a Shimatzu UV 1601 spectrophotometer and diluted with DMEM-1% FCS to obtain the desired concentrations.

### 3.6. Intracellular localization of each amino acid porphyrins conjugates

The cells were seeded onto coverslips placed into 24-well plates at densities of $3 \times 10^4$ (HaCaT and HeLa cells) and allow to grow for 24 h. After that, cells were incubated with the liposomal suspension of porphyrins amino acid conjugates for variable times. The samples were washed twice with PBS and then were mounted onto slides with PBS. Samples were studied under fluorescence microscopy.

### 3.7. Photodynamic therapy treatment in vitro

Cells seeded in 24-well plates were incubated with an appropriate volume of each porphyrin amino acid conjugate, incorporated into liposomes; 4 h after started the treatment, irradiations were performed. After irradiations, the medium was replaced by fresh complete medium without drugs and the cells were incubated in dark for another 24 h and then tested their viability.

### 3.8. Light source

A LED array was constructed and used for irradiation. It is composed of a matrix of 24 × 16 LEDs (Kingbright, model L53 SRCE), which makes a total of 384 light sources with an emission peak

at 654 nm and a bandwidth at half maximum (BWHM) of ±20 nm, as measured with a spectrometer (Fiberoptic, Avantes). The array works with alternate current, fed by integrated circuits (MBI 6001 N2D, Macroblock Inc.), which provide current pulses of 1.66 ms duration, followed by a non-emitting period of 7 ms. So the emission of the LED array has a pulsed light pattern. The irradiance at 1.5 cm distance from the array surface is 9.15 mW/cm$^2$ (photocell PAR 190 Li-1000, Li-Cor).

### 3.9. MTT viability assay

Phototoxicity and cell viability were documented by the MTT assay.[39] Following appropriate treatments, 3-[4,5-dimethylthiazol-2-yl]-2,5-diphenyltetrazolium-bromide (MTT) solution was added to each well at a concentration of 0.5 ng/mL, and plates were incubated at 37 °C for 2–3 h. The resulting formazan crystals were dissolved by the addition of DMSO and absorbance was measured at 560 nm. The viability was also established by microscopy with a trypan blue exclusion test using a Neubauer chamber counter. In both cases, similar results were obtained. The same procedure was carried out without irradiation for determining dark toxicity.

### 3.10. Cell morphology

Changes in cell morphology were analyzed using bright field illumination. After PDT treatments the cells were fixed with methanol at −2 °C for 10 min. After three washes with PBS, cells were stained with toluidine blue (TB, Merck, Darmstadt, Germany) (0.5 mg/mL in distilled water, 5 min). After being washed and air-dried, preparations were mounted in DePeX (Serva, Heidelberg, Germany) and observed under bright field illumination.

## Acknowledgments

Thanks are due to Fundação para a Ciência e a Tecnologia (FCT, Portugal) and POCI (FEDER) for funding the Organic Chemistry Research Unit. V. Vaz Serra also thanks FCT for Ph.D. Grant (SFRH/BD/28122/2006).

## References and notes

1. Dougherty, T. J.; Gomer, C.; Henderson, B. W.; Jori, G.; Kessel, D. *J. Natl. Cancer Inst.* **1998**, *90*, 889.
2. Handerson, B. W.; Dougherty, T. *J. Photochem. Photobiol.* **1992**, *55*, 145.
3. Brown, S.; Brown, E. A.; Walker, I. *Lancet Oncol.* **2004**, *5*, 497.
4. *The Porphyrin Handbook*; Kadish, K. M., Smith, K. M., Guillard, R., Eds.; Academic Press: San Diego, 2000; Vol. 6,.
5. DeRosa, M. C.; Crutchley, R. J. *Coord. Chem. Rev.* **2002**, 351.
6. MacDonald, I.; Dougherty, T. J. *J. Porphyrins Phthalocyanines* **2001**, *5*, 105.
7. Allison, R. R.; Downie, G. H.; Cuenca, R.; Xin-Hua, H.; Childs, C. J. H.; Sibat, C. H. *Photodiag. Photody. Ther.* **2004**, *1*, 27.
8. *Chemical Aspects of Photodynamic Therapy*; Bonnett, Ed.; Gordon and Breach Science Publishers: Amsterdam, 2000; pp 173–174.
9. Castano, A. P.; Deminova, T. N.; Hamblin, M. R. *Photodiag. Photody. Ther.* **2004**, *1*, 279.
10. Cavanaugh, P. G. *Breast Cancer Res. Treat.* **2002**, *72*, 117.
11. Sutton, J. M.; Clarke, O. J.; Fernandez, N.; Boyle, R. W. *Bioconjugate Chem.* **2002**, *13*, 249.
12. Hamblin, M. R.; Miller, J. L.; Ortel, B. *Photochem. Photobiol.* **2000**, *72*, 533.
13. Nagae, T.; Louie, A. Y.; Aizawa, K.; Ishimaru, S.; Wilson, S. E. *J. Cardiovasc. Surg. (Torino)* **1998**, *39*, 709.
14. Chaloin, L.; Bigey, P.; Loup, C.; Marin, M.; Galeotti, N.; Piechaczyk, M.; Heitz, F.; Meunier, B. *Bioconjugate Chem.* **2001**, *12*, 691.
15. Rahimipour, S.; Ben-Aroya, N.; Ziv, K.; Chen, A.; Fridkin, M.; Koch, Y. *J. Med. Chem.* **2003**, *46*, 3965.
16. De Luca, S.; Tesauro, D.; Di Lello, P.; Fattorusso, R.; Saviano, M.; Pedone, C.; Morelli, G. *J. Pept. Sci.* **2001**, *7*, 386.
17. Sibrian-Vazquez, M.; Jensen, T. J.; Fronczek, F. R.; Hammer, R. P.; Vicente, M. G. H. *Bioconjugate Chem.* **2005**, *16*, 852.
18. Cavaleiro, J. A. S; Faustino, M. A. F; Tomé, J. P. C In *Carbohydrate Chemistry*; Rauter, A. P., Lindhorst, T. K., Eds.; Chemical and Biological Approaches; RSC Publishing: Cambridge, 2009; Vol. 35, pp 199–227.
19. Perrée-Fauvel, M.; Verchére-Béaur, C.; Tarnaud, E.; Anneheim-Herbelin, G.; Bône, N.; Gaudemer, A. *Tetrahedron* **1996**, *52*, 13569.
20. Biron, E.; Voyer, N. *Chem. Commun.* **2005**, 4652.
21. Kwitniewski, M.; Kunikowska, D.; Dera-Tomaszewska, B.; Tokarska-Pietrzak, E.; Dziadziuszko, H.; Graczyk, A.; Glosnicka, R. *J. Photochem. Photobiol., B -Biol.* **2005**, *81*, 129.
22. Schneider, R.; Tirand, L.; Frochot, C.; Vanderesse, R.; Thomas, N.; Gravier, J.; Guillemin, F.; Barberi-Heyob, M. *Anticancer Agents Med. Chem.* **2006**, *6*, 469.
23. Wang, H. M.; Jiang, J. Q.; Xiao, J. H.; Gao, R. L.; Lin, F. Y.; Liu, X. Y. *Chem. Biol. Interact.* **2008**, *172*, 154.
24. Tomé, J. P.; Neves, M. G.; Tomé, A. C.; Cavaleiro, J. A. S.; Soncin, M.; Magaraggia, M.; Ferro, S.; Jori, J. *J. Med. Chem.* **2004**, *47*, 6649.
25. Soukos, N. S.; Hamblin, R.; Hasan, T. *Photochem. Photobiol.* **1997**, *65*, 773.
26. Hamblin, R.; O'Donnel, D.; Murthy, N.; Rajagopalan, K.; Michaud, N.; Sherwood, M.; Hasan, T. *J. Antimicrob. Chemother.* **2002**, *49*, 941.
27. Vaz Serra, V.; Faustino, M. A. F.; Tomé, J. P. C.; Pinto, D. C. G. A.; Neves, M. G. P. M. S.; Tomé, A. C.; Silva, A. M. S.; Cavaleiro, J. A. S.; Camões, F.; Vieira, S. I.; Da Cruz e Silva, E. F. *Acta Chim. Slov.* **2009**, *56*, 603.
28. Faustino, M. A. F.; Neves, M. G. P. M. S.; Cavaleiro, J. A. S.; Neumann, M.; Brauer, H.-D.; Jori, G. *Photochem. Photobiol.* **2000**, *72*, 217.
29. Faustino, M. A. F.; Neves, M. G. P. M. S.; Vicente, M. G. H.; Cavaleiro, J. A. S.; Neumann, M.; Brauer, H.-D.; Jori, G. *Photochem. Photobiol.* **1997**, *66*, 405.
30. Rocha Gonsalves, A. M.; Varejão, J. M. T. B.; Pereira, M. M. *J. Heterocycl. Chem.* **1991**, *28*, 635.
31. Vaz Serra, V.; Domingues, M. R. M.; Faustino, M. A. F.; Tomé, J. P. C.; Neves, M. G. P. M. S.; Tomé, A. C.; Cavaleiro, J. A. S. *Rapid Commun. Mass Spectrom.* **2005**, *19*, 2569.
32. Bonnett, R.; Martinez, G. *Tetrahedron* **2001**, *57*, 9513.
33. Mitzel, F.; FitzGerald, S.; Beeby, A.; Faust, R. *Eur. J. Org. Chem.* **2004**, 1136.
34. Oda, K.; Ogura, S.; Okura, I. *J. Photochem. Photobiol., B* **2000**, *59*, 20.
35. Spiller, W.; Kliesch, H.; Wöhrle, D.; Hackbarth, S.; Röder, B.; Schnurpfeil, G. *J. Porphyrins Phthalocyanines* **1998**, *2*, 145.
36. Gerhardt, S. A.; Lewis, J. W.; Zhang, J. Z.; Bonnett, R.; McManus, K. A. *Photochem. Photobiol. Sci.* **2003**, *2*, 934.
37. Stockert, J. C.; Juarranz, A.; Villanueva, A.; Nonellm, S.; Horobin, R. W.; Soltermann, A. T.; Durantini, E. N.; Rivalona, V.; Colombo, L. L.; Espada, J.; Cañete, M. *Curr. Top. Pharmacol.* **2004**, *8*, 185.
38. Juarranz, A.; Espada, J.; Stockert, J. C.; Villanueva, A.; Polo, S.; Dominguez, V.; Cañete, M. *Photochem. Photobiol.* **2001**, *73*, 283.
39. Merlin, J. L.; Azzi, S.; Lignon, D.; Ramacci, C.; Zeghari, N.; Guillemin, F. *Eur. J. Cancer* **1992**, *28*, 1452.